

Silicon light emitters and amplifiers: state of the art

Lorenzo Pavesi

Dipartimento di Fisica, via Sommarive 14, 38050 Povo (Trento), Italy

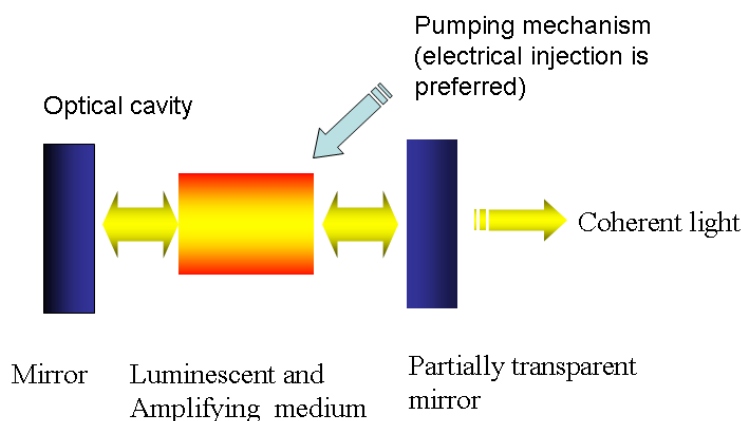
ABSTRACT

In this paper a review of the reported approaches to achieve an injection Silicon laser is presented. After an initial discussion of the basic on light amplification and gain in semiconductor, we consider the limitations of silicon, in particular its band structure. Then the various approaches to get an injection silicon laser are presented and evaluated: bulk silicon, silicon nanocrystals, Er coupled silicon nanocrystals.

Keywords: Silicon photonics, Laser, Erbium, Nanocrystals, Optical gain, Stimulated emission, Light emitting devices

1. INTRODUCTION

Silicon photonics, where photonic devices are produced by using standard microelectronic facilities, is a technology which has shown several improvements and breakthroughs in these last years. Convergence between electronics and photonics on a very same semiconductor chip, i. e. between computation and communication, is possible with silicon photonics. Both passive and active optical functionalities have been made possible in silicon. An example is fast optical modulation, which was considered impossible in Si due to the lack of any electro-optical effects, but which has been demonstrated at the high speeds needed for nowadays communication. Even a room temperature, continuous wave, optically pumped silicon laser has been demonstrated. The only still lacking device is an injection silicon laser. However even though the device has not yet been demonstrated, several competing routes have been suggested and very interesting results published in the literature. In this paper I will try to make the point of the worldwide research effort to build an injection silicon laser.



$$\text{Round trip gain } R^2G^2 > 1$$

Figure 1. Basic components of a laser

This article is an up-to-date version of a chapter published in *Optical Interconnects: the silicon approach*, ed. by L. Pavesi and G. Guillot, Springer-Verlag (2006)
E-mail: lorenzo.pavesi@unitn.it

2. BASIC ON LIGHT AMPLIFICATION AND GAIN

A laser is based on three main components (Fig. 1): an active material which is able to generate and to amplify light by stimulated emission of photons, an optical cavity which provides the optical feed-back to sustain the laser action, and a pumping mechanism which is able to excite the active material such that population inversion can be achieved [1]. In an injection diode laser the pumping mechanism is provided by carrier injection via a p-n junction and the optical feedback is provided by a Fabry-Perot cavity. The use of electrical injection makes the device particularly interesting for integration with microelectronics.

The light generation property of an active material is quantified by the internal quantum efficiency η_{int} . η_{int} gives the ratio between the number of photons generated times the number of electron-hole pairs that recombine. This number is given by the ratio between the electron-hole (e-h) radiative recombination probability over the total e-h recombination probability, i. e. by the fraction of all the excited e-h pairs that recombine radiatively. It easy to demonstrate that $\eta_{int} = \tau_{nr} / (\tau_{nr} + \tau_r)$, where τ_{nr} and τ_r are the non-radiative and radiative lifetimes, respectively. Thus in order to have an high η_{int} either the radiative lifetime should be short (as in direct bang-gap semiconductors) or the non-radiative lifetime should be long (as in color center systems).

The property of amplifying light is given by the gain spectrum of the material. For a bulk semiconductor it is related to the joint density of states $\rho(\hbar\omega)$, the Fermi inversion factor $f_g(\hbar\omega)$ and the radiative lifetime:

$$\begin{aligned} g(\hbar\omega) d\Phi(\hbar\omega) &= dr_{stim}(\hbar\omega) - dr_{abs}(\hbar\omega) \\ &= \frac{\lambda^2}{8\pi\tau_r} \rho(\hbar\omega) f_g(\hbar\omega) \Phi(\hbar\omega) dz \end{aligned} \quad (1)$$

where g is the gain coefficient, $d\Phi$ the change in the photon flux, dr_{stim} or dr_{abs} the rate of stimulated emission or absorption at a given photon energy $\hbar\omega$, respectively, $f_g(\hbar\omega, E_F^e, E_F^h, T) = [f_e(\hbar\omega, E_F^e, T) - (1 - f_h(\hbar\omega, E_F^h, T))]$, f_e and f_h are the thermal occupation functions for electrons and holes, and Φ the photon flux density. E_F^e and E_F^h are the quasi-Fermi level for electrons and holes, respectively. When no external pumping is present, the Fermi inversion factor reduces to the simple Fermi statistics for an empty conduction band and a filled valence band ($f_g < 0$) and the gain coefficient reduces to the absorption coefficient α . When an external pump excites a large density of free carriers, the splitting of the quasi-Fermi levels increases and when $E_F^e - E_F^h > \hbar\omega$ the condition of population inversion is verified and $f_g > 0$. This means that Eq. (1) is positive and hence the system shows positive net optical gain ($g > 0$). Note that in eq. (1) a critical role is played by the radiative lifetime: the shorter the lifetime the stronger the gain.

For an atomic system, the expression of the gain coefficient reduces to

$$g(\hbar\omega) = \sigma_{em}(\hbar\omega) N_2 - \sigma_{abs}(\hbar\omega) N_1 \quad (2)$$

where σ_{em} is the emission cross section, σ_{abs} the absorption cross section, N_2 and N_1 the density of active centers in the excited and ground states, respectively. If $\sigma_{em} = \sigma_{abs}$, the condition to have positive optical gain is that $N_2 > N_1$, i. e. the condition of population inversion.

If a piece of active material of length L is used to amplify light, one achieves light amplification whenever the material gain g is positive *and* larger than the propagation losses α_p of the light trough the material, that is $g > 0$ and $g > \alpha_p$. If the system is forged as a waveguide L long, and we call I_T and I_0 the intensity of the transmitted and of the incident beams, the amplification factor of the light is then

$$G = I_T / I_0 = \exp[(\Gamma g - \alpha_p) L] > 1. \quad (3)$$

where Γ is the optical confinement factor of the optical mode in the active region.

In a laser, optical feedback is usually provided by a Fabry-Peròt cavity so that the round trip gain (the overall gain experienced by a photon travelling back and forth across the cavity) can be larger than 1. This condition is expressed by the relation $G^2 R_1 R_2 > 1$, where R_1 and R_2 are the back and front mirror reflectivities.

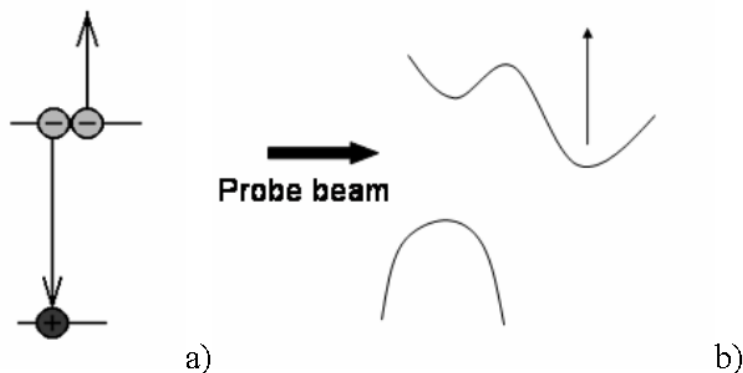


Figure 2. a) Auger process. b) free carrier absorption process. The wavy lines represent the band structure of silicon

3. LIMITATION OF SILICON FOR LIGHT AMPLIFICATION

Among the various semiconductor materials which have been used to form lasers, it is striking the absence of Silicon. Let us review why Si has not been used as a laser materials [2,3,4]. Si is an indirect band-gap semiconductor. As a consequence, the probability for a radiative recombination is low, which in turn means that the e-h radiative lifetime is long, of the order of some milliseconds. An e-h pair has to wait in average a few milliseconds to recombine radiatively. During this time both the electron and the hole move around and cover a volume of the order of $10 \mu\text{m}^3$. If they encounter a defect or a trapping centre, the carriers might recombine non-radiatively. Typical non-radiative recombination lifetimes in Si are of the order of some nanoseconds. Thus, in electronic grade silicon the internal quantum efficiency η_{int} is about 10^{-6} . This is the reason why silicon is a poor luminescent material: the efficient non-radiative recombinations which deplete rapidly the excited carriers. Many strategies have been researched over the year to overcome this silicon limitation, some of which are based on the spatial confinement of the carriers, other on the introduction of impurities, other on the use of quantum confinement, others on the use of Si-Ge alloys or superlattices [2].

In addition, two other phenomena limit the use of Si for optical amplification (see Fig. 2). The first is a non-radiative three-particles recombination mechanism where an excited electron (hole) recombines with an hole (electron) by releasing the excess energy to another electron (hole). This is called non-radiative Auger recombination mechanism (Fig. 2a). This recombination mechanism is active as soon as more than one carrier is excited. The probability of an Auger recombination is directly proportional to the number of excited carriers and inversely proportional to the band-gap energy [5]. For our discussion this is a very relevant mechanism because the more excited is the semiconductor the more the Auger recombination is effective. The probability for an Auger recombination in a bulk material is proportional to Δn^3 , we can thus write a non-radiative recombination lifetime due to Auger as $\tau_A = 1/C\Delta n^2$, where C is a constant which depends on the doping of the material. For silicon $C \sim 10^{-30} \text{ cm}^6\text{s}^{-1}$ [5]. For $\Delta n \sim 10^{19} \text{ cm}^3$, $\tau_A = 10 \text{ ns}$. The Auger recombination is the dominant recombination mechanism for high carrier injection rate in Si.

The second phenomenon is related to free carrier absorption (see Fig. 2b). Excited carriers might absorb photons and thus deplete the inverted population and, at the same time, increase the optical losses suffered by the signal beam. The free carrier absorption coefficient can be empirically related to the Si free carrier density n_{fc} and to the light wavelength λ as $\alpha_n \sim 10^{-18} n_{fc} \lambda^2$ at 300 K [6]. For $n_{fc} = 10^{19} \text{ cm}^{-3}$ and $\lambda = 1.55 \mu\text{m}$, $\alpha_n = 24 \text{ cm}^{-1}$. For heavily doped Si this is the main limitations to lasing, while for intrinsic Si this contribution can be exceedingly small, unless n_{fc} is very high as in a laser. In confined system, such as Si nanocrystals, this recombination mechanism is due to confined carriers and, hence, is called confined carrier absorption.

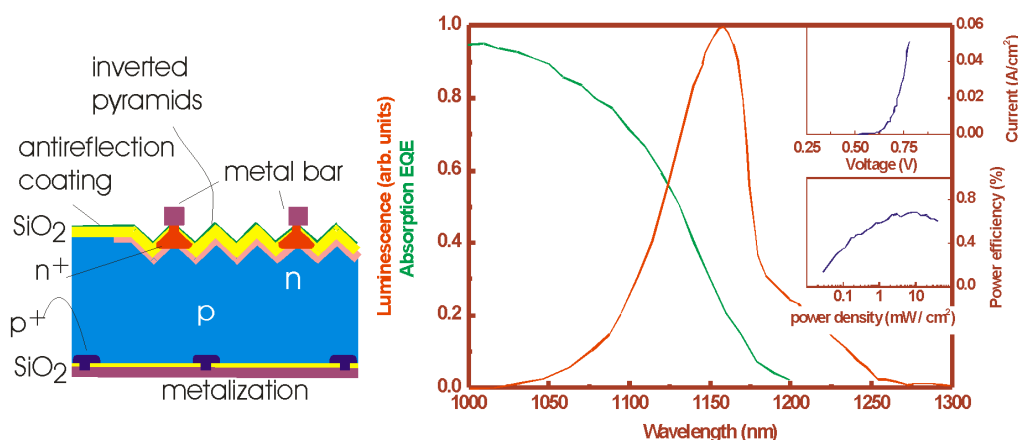


Figure 3. Summary of the results of the Australian group on a bulk silicon LED. Left: sketch of the LED geometry. Right: Luminescence spectrum (red), absorption spectrum (green), power efficiency vs injected electrical power density (blue) and I-V characteristics (inset) at room temperature. Data have been redrawn from Ref. 9,13.

4. VARIOUS APPROACHES TO A SILICON LASER

In early 2000 a series of papers appeared that questioned the common believe that silicon cannot be used to form a laser [7-10]. In October 2004 the first report on a silicon laser appeared [11], while in February 2005 the first CW Raman laser integrated in silicon was reported [12].

4.1. Bulk Silicon light emitting diodes

The common believe that bulk silicon cannot be a light emitting material has been severely questioned in a series of recent works. One was published in 2001 [9]. An Australian group noticed that world-record solar cells are characterized by extremely long carrier recombination lifetimes of the order of some milliseconds. That is, the recombination lifetime is of the order of the radiative lifetime, hence η_{int} is of the order of 1. Then, if the solar cell is biased in the forward regime instead of the usual reverse regime, the solar cell could behave as a very efficient light emitting diode.

Fig. 3 shows a schematic of the device and a room temperature emission spectrum. To increase the light extraction efficiency, the LED surface was texturized so that most of the internally generated light was impinging on the external surface of the cell with an incident angle lower than the critical angle for total internal refraction. Thus the light extraction efficiency was increased from a few % typical of a flat surface to almost 100% for the texturized LED. Finally, to reduce free carrier absorption to a minimum, the electrodes, i. e. the heavily doped regions, were confined in very thin and small lines. By using these three practices, a plug-in efficiency (ratio of the optical power emitted from the LED to the electrical driving power) larger than 1% at 200 K was achieved. Most interesting the turn-on voltage of the device was the same as the forward bias of the solar cell, i. e. less than 1 V.

The same research group published also a theoretical paper [14] which questioned one common believe that indirect band-gap materials could not show optical gain because of parasitic absorption processes due to free carrier [15]. Indeed they demonstrate that optical gain is theoretically possible and pointed out that the most suitable energy region is the sub-band gap region where processes involving phonons could help in achieving gain.

These theoretical arguments have been partially confirmed in a recent study where stimulated emission has been observed (see Fig. 4) [16]. As the limit to efficient light generation in Si is the short non-radiative lifetime,

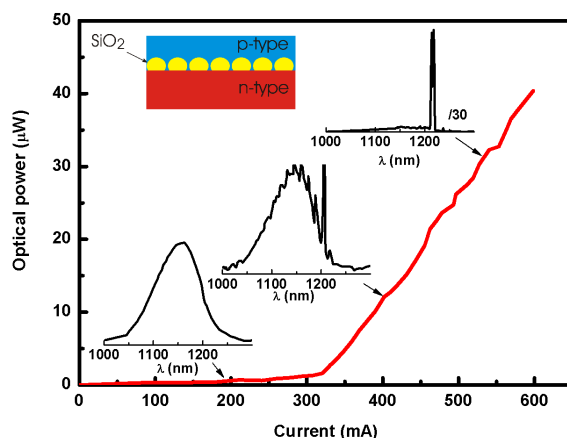


Figure 4. Optical power versus injected current for a LED containing SiO₂ nanoclusters in the junction region (inset). Also shown are a few electroluminescence spectra for different injection rate (arrows). The data have been redrawn from Ref. 16.

the idea was to avoid carrier diffusion and to spatially localize free carriers in a small device region where non-radiative recombination centres can be easily saturated.

Carrier localization was achieved by spin-on doping of small silica nanoparticles at the junction of a p-n diode (fig. 4) [16]. The current-voltage I-V characteristic of the diode shows rectifying behavior with a clear threshold in the light-current L-I characteristic. A change from a broad emission spectrum characteristic of band-to-band emission below threshold to sharp peaks due to stimulated emission above threshold is observed too. Stimulated emission is observed for a two-phonon indirect transition as it was theoretically predicted. Furthermore, when the injection current significantly exceeds the threshold, a single peak dominates. All these results are very encouraging since the proposed system have excellent electrical qualities as they are p-n junctions.

Recently, another report of stimulated emission in bulk silicon has appeared [10]. Nanopatterning of a thin silicon on insulator layer allows to have a large effective silicon surface where a sizable density of A' centers could pile-up. These defect centers are believed to play the role of active optical centers which can be optically inverted. Indeed very convincing experimental data of gain in these nanopatterned films have been reported. The major caveat is that the gain is vanishing as the temperature is raised: sizable gain is observed only for temperatures lower than 80K.

4.2. Optical gain in Silicon nanocrystals

Another interesting approach to form light emitters and amplifiers in Si is to use small Si nanoclusters (Si-nc) dispersed in a dielectric matrix, most frequently SiO₂ [2]. With this approach one maximizes carrier confinement, improves the radiative probability by quantum confinement, shifts the emission wavelength to the visible and controls the emission wavelength by Si-nc dimension, decreases the confined carrier absorption due to the decreased emission wavelength, and increases the light extraction efficiency by reducing the dielectric mismatch between the source materials and the air. Various techniques are used to form Si-nc whose size can be tailored in the few nm range (Fig. 5).

Starting by a silicon rich oxide, which can be formed by deposition, sputtering, ion implantation, cluster evaporation, etc., a partial phase separation is induced by thermal annealing. The duration of the thermal treatment, the annealing temperature, the starting excess Si content are all determining the final sizes of the cluster, their dispersion in size which can be significant and the Si-nc crystalline nature. The size dispersion is usually claimed as the source of the broad emission lineshape that at room temperature is typical of the

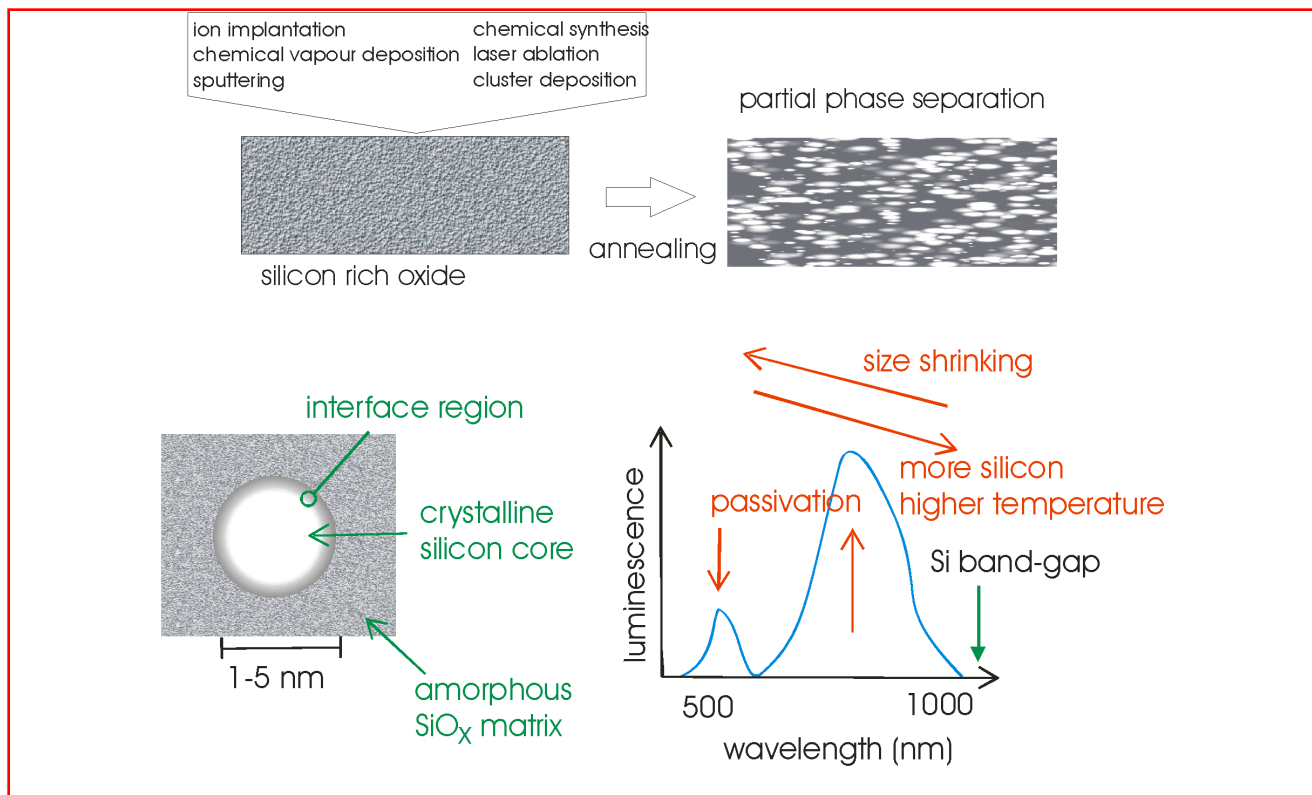


Figure 5. Si nanocrystals formation, structure and luminescence spectrum

Si-nc emission spectra. However both size selected deposition [17] and single Si-nc luminescence experiments [18], demonstrate that most of the luminescence broadening is intrinsic in nature. The active role of the interface region in determining the optical properties of Si-nc has been highlighted in a joint theoretical and experimental paper [19]. The origin of the luminescence in Si-nc is still unclear, many authors believe that it comes from confined exciton recombination in the Si-nc [20] while others support a defect assisted recombination mechanism where luminescence is due to recombination of carriers trapped at radiative recombination centres which form at the interface between Si-nc and the dielectric [21] or even in the dielectric [22]. One candidate for these centres is the silanone bond which is formed by a double Si-O bonds [23]. The most probable nature of the luminescence in Si-nc is a mechanism which involves both recombination paths: excitons at about 800 nm and trapped carriers on radiative interface state at about 700 nm. Indeed passivation experiments show that the intensity and lineshape of the emission can be influenced by exposition to hydrogen gas or by further oxidation [24].

A number of papers reported observation of optical gain in these systems. [7,25-32] Fig. 6 reports a summary of the most relevant data taken on Si-nc formed by plasma enhanced chemical vapor deposition (PECVD). [25-27] Two techniques are here reported: the variable stripe length method (VSL) which is sketched in the inset of Fig. 6 and is based on the one-dimensional amplifier model [26], and the pump-probe technique which is based on the probe amplification in presence of an high energy and high intensity pump beam [27]. In the VSL method by varying the pumped region extent (whose length is z) one measures the amplified spontaneous emission (I_{ASE}) signal coming out from an edge of a waveguide whose core is rich in Si-nc:

$$I_{ASE}(z) = \frac{J_{sp}(\Omega)}{g_{mod}} (e^{g_{mod} z} - 1)$$

where $J_{sp}(\Omega)$ is the spontaneous emission intensity emitted within the solid angle Ω and g_{mod} is the net modal gain of the material, defined as $g_{mod} = \Gamma g_m - \alpha$.

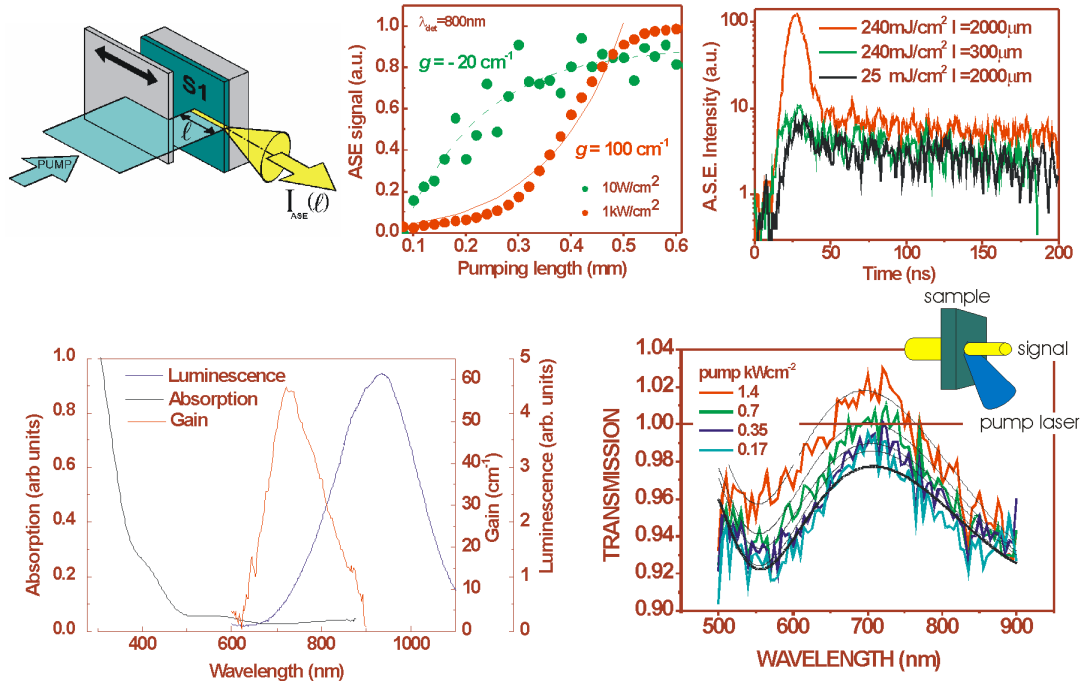


Figure 6. Summary of various experimental proofs of gain in Si-nc. Top left panel, geometry used to measure the ASE, amplified spontaneous emission; top center panel, ASE versus the pumping length for two pumping powers; top right, ASE time decay for the various pumping conditions indicated in the inset (l is the pumping length); bottom left, luminescence, absorption and gain spectra at room temperature for a Si-nc rich waveguide; bottom right, transmission spectra for various pumping powers (the inset shows the experimental geometry used). Data have been redrawn from Ref. 25, 26 and 27

Data reported in Fig. 6 shows that the ASE intensity increases sublinearly with the pumping length when the pumping power is lower than a threshold. For pumping power higher than threshold the ASE signal increases more than exponentially. This is a consequence of the pump induced switching from absorption ($g_{mod} < 0$) to gain ($g_{mod} > 0$).

In addition if time resolved measurements are performed (Fig 6 right top panel), [27] the ASE decay lineshape shows two time regimes: a fast decay within the first ns and a slow time decay with typical time constant of few μs . It is well known that Si-nc have time decay constant of some μs , so the appearance of a ns time decay is at first surprising. What is important is the fact that the fast decay appears only if the pumping power and the excitation volume are both large. If one decrease the excitation volume at high power or the pumping power at large excitation volume the fast decay disappears. This can be understood if the fast decay is due to stimulated emissions. In fact, at high pumping rate three competitive paths open: stimulated emission, Auger recombination and confined carrier absorption. All these could be the cause of the fast decay. In particular, the Auger lifetime and the confined carrier absorption lifetime can be modelled in a Si-nc by $\tau_A = \frac{1}{C_A} N_{ex}$ and $\tau_{CC} = \frac{1}{2C_{CC} N_{ex}}$, where C_A and C_{CC} are coefficients and N_{ex} is the density of excited recombination centers. N_{ex} is directly proportional to the pumping power and not to the pumping volume. Thus decreasing the pumping length the ASE lineshape should be unchanged. On the other hand, by a simple rate equation modelling,[33] the stimulated emission lifetime turns out to be $\tau_{se} = \frac{4}{3} \pi R_{NS}^3 \frac{1}{\xi \sigma_g c n_{ph}}$, where R_{NS} is the average radius of the Si-nc, ξ their packing density, σ_g the gain cross section and n_{ph} the photon flux density. Note that τ_{se} depends on the material properties (R_{NS}, ξ, σ_g) but also on the photon flux density n_{ph} which exists in the waveguide.

n_{ph} depends, in turn, on the waveguide losses, the Si-nc quantum efficiency and the pumping rates. In addition if the sample shows gain, by increasing the excitation volume, n_{ph} exponentially increases, i.e. τ_{se} decreases. τ_{se} shortens when either the pumping length or the pumping power are increases as both increase n_{ph} . It is important to notice that calculations show that the Auger lifetime in Si-nc are in the interval 0.1-10 ns,[34] which means that Auger is a strong competitive process which should be always considered. In some Si-nc systems, due to either material problems or poor waveguide properties or both, Auger and confined carrier absorption might prevails and no optical gain could be observed.

Fig. 6 bottom left shows a summary of the wavelength dependence of the luminescence, absorption and gain spectra in a sample with 4 nm Si-nc [25]. It is seen that the gain spectrum is on the high energy side of the emission band and that absorption is negligible in the region of gain and luminescence. These facts suggest a four level models to explain the gain where the levels can be associated to both different Si-nc populations or to a radiative state associated to a Si=O double bond for which optical excitation causes a large lattice relaxation of the Si=O bond[35] as in the silanone molecule. Pump-probe measurements were attempted with contradictory results world wide [27,36] Our group was able to show probe amplification under pumping conditions (see Fig. 6 bottom right panel) [27], while another group reported pump-induced absorption probably associated with confined carrier absorption [36]. Literature results show that the confined carrier absorption cross section σ_{fc} in Si-nc is at least one order of magnitude reduced with respect to bulk Si [37]: $\sigma_{fc} \approx 10^{-18} \text{ cm}^2$ at 1.55 μm in P-doped Si-nc. This cross section should be further reduced at 700 nm due to the λ^2 dependence of the confined carrier absorption. Transmission measurements of a probe beam through a Si-nc slab deposited on a quartz substrate show the typical interference fringes due to multiple reflection at the slab interfaces (Fig. 6). When the pump power is raised the transmission is increased and, at the maximum power used, net probe amplification with respect to the input probe intensity in air is observed in a narrow wavelength interval. Note that the probe amplification spectrum overlaps the fast luminescence spectrum measured by time resolved technique. Based on these results, design of optical cavity for a Si-nc laser has been published [38]. In addition very favorable results have been published with respect to Si-nc based LED where turn on voltage as low as few volts can be demonstrated by using thin Si-nc active layers [39]. Electroluminescence in these LED was due to impact excitation of electron-hole pairs in the Si-nc. Another recent work [40] reports on a FET structure where the gate dielectric is rich of Si-nc. In this way by changing the sign of the gate bias, separate injection of electrons and holes in the Si-nc is achieved. Luminescence is observed only when both electrons and holes are injected into the Si-nc. By using this pulsing bias technique, high efficiency in the emission of the LED is achieved due to the co-presence of electrons and holes. Channel optical waveguide with a core layer rich of Si-nc show optical losses of only a few dB/cm mainly due to direct Si-nc absorption and to scattering caused by the composite nature of the guiding medium [41]. All these different experiments have still to be merged in a laser cavity structure to demonstrate a Si-nc based laser.

4.3. Light amplification in Er coupled Si nanoclusters

The radiative transitions in the internal 4f shell of Erbium ions (Er^{3+}) are exploited in the erbium doped fiber amplifier (EDFA) [42]: an all optical amplifier which has revolutionized the optical communication technology. During the nineties several experimental efforts have been spent in order to develop an efficient and reliable light source by using Er^{3+} in Si [2]. The idea was to excite the Er^{3+} , which emits 1.535 μm photons, by an energy transfer from the electrically injected e-h pairs in a p-n Si diode. The most successful results have been the demonstration of room temperature emission with an external quantum efficiency of 0.1 % in a MHz modulated Er^{3+} doped Si LED [43]. The main problem associated to Er^{3+} in Si is the back transfer of energy from the Er^{3+} ions to the Si host, which causes a lowering of the emission efficiency of the diode [44]. This is due to a resonant level which appears in the Si band gap due to the Er^{3+} doping and which couples with the Er^{3+} levels. In order to reduce this back-transfer process it was proposed to enlarge the band-gap of the Er^{3+} host so that the resonance between the defect level and the internal Er^{3+} levels is lost [45]. Si-nc in a SiO_2 dielectric were thus proposed as the host [46]. Indeed it turns out that Si-nc are very efficient sensitizers of the Er^{3+} luminescence with typical transfer efficiency as high as 70% and with a typical transfer time of 1 μs [47]. In addition, the Er^{3+} are dispersed in SiO_2 , where they found their most favorable chemical environment. Quite interestingly the transfer efficiency gets maximized when the Si-nc are not completely crystallized but still in the form of Si

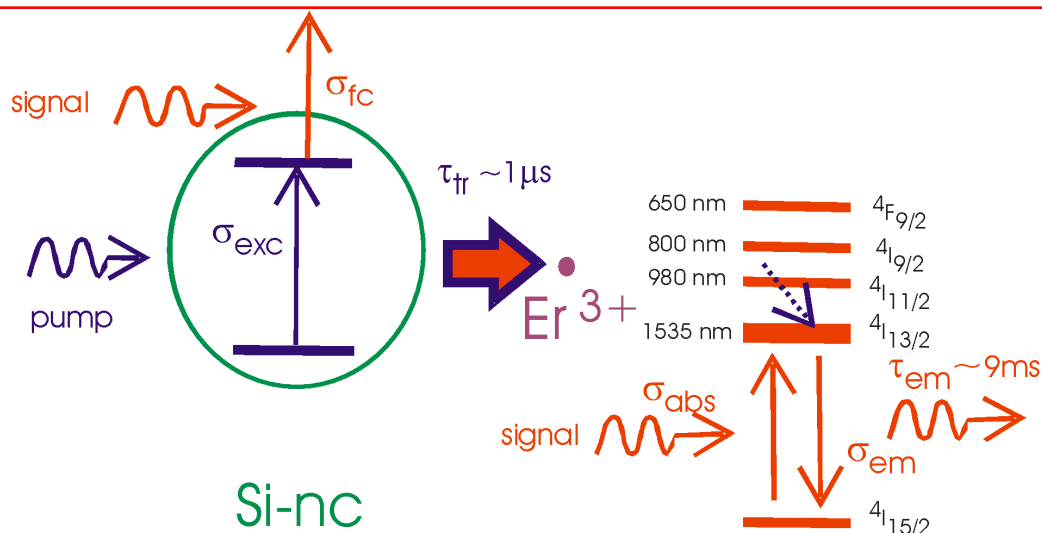


Figure 7. Diagram of the excitation process of Er^{3+} ions via a Si-nc, with the main related cross sections. On the left the main internal energy levels of the Er^{3+} are shown.

nanoclusters [48]. Some reports claim even that the Er^{3+} can be excited through defects in the matrix [49]. Still under debate is the number of Er ions that can be excited by a single Si-nc: a few or many ions.

Fig. 7 summarizes the various mechanisms and defines the related cross-sections for this system. Excitation of Er^{3+} occurs via an energy transfer from photoexcited e-h pairs which are excited in the Si-nc: the overall efficiency of light generation at $1.535 \mu\text{m}$ through direct absorption in the Si-nc is described by an effective Er^{3+} excitation cross section σ_{exc} . On the other hand, the direct absorption of the Er^{3+} ions, without the mediation of the Si-nc, and the emission from the Er ions are described by an absorption σ_{abs} and an emission σ_{em} cross sections, respectively. The typical radiative lifetime of Er^{3+} is of 7 ms, which is similar to the one of Er^{3+} in pure SiO_2 [50]. Fig. 8 left reports the luminescence and the absorption spectra measured in an Er^{3+} coupled Si-nc ridge waveguide at room temperature [51].

Table 1. Summary of the various cross sections related to Er^{3+} in various materials. The best reported results are shown and are taken in the reference listed in the last column.

	Er in SiO_2 (cm^2)	Er in Si (cm^2)	Er in Si-nc (cm^2)	Reference for Er in Si-nc
Effective excitation cross section of luminescence at a pumping energy of 488 nm	$1-8 \times 10^{-21}$	3×10^{-15}	$1.1-0.7 \times 10^{-16}$	52,53
Effective excitation cross section of electroluminescence		4×10^{-14}	1×10^{-14} by impact ionization	54
Emission cross section at $1.535 \mu\text{m}$	6×10^{-21}		1×10^{-20}	51
Absorption cross section at $1.535 \mu\text{m}$	4×10^{-21}	2×10^{-20}	1×10^{-20}	51

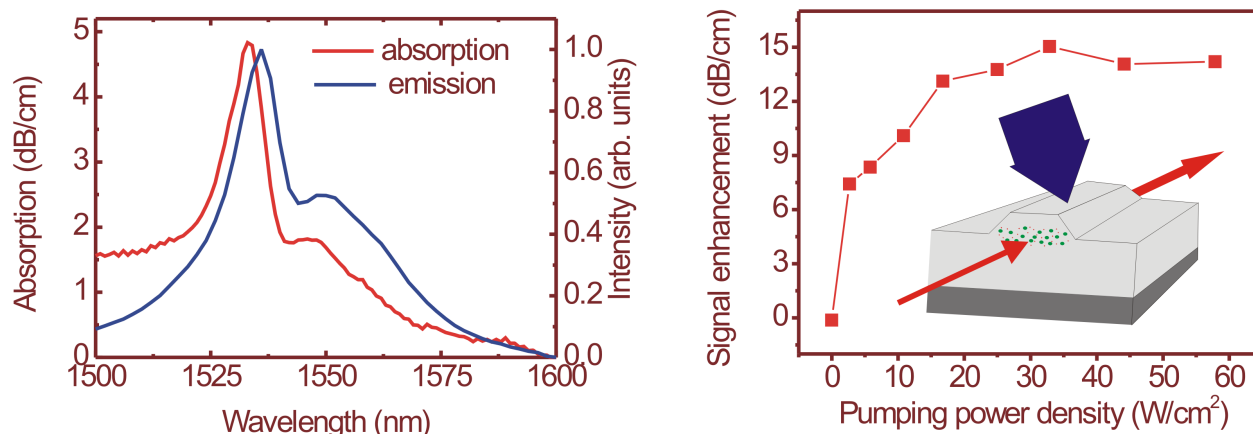


Figure 8. (left) Absorption and luminescence spectra of an Er^{3+} coupled Si-nc waveguide. Data after Ref.51 (right) Signal enhancement at $1.535 \mu\text{m}$ in an Er^{3+} coupled Si-nc waveguide versus the pumping power density by using top pumping as shown in the inset. Data after Ref. 55.

Table 1 summarizes the best results for the various cross sections reported in the literature. It is important to notice the five order of magnitude increase in σ_{exc} and the fact that this value is conserved also when electrical injection is used to excite the Si-nc [54]. In addition, it is striking that σ_{em} gets enhanced by one order of magnitude with respect to the value for Er^{3+} in pure SiO_2 [56]. A cautious note should here drawn as measurements for σ_{abs} do not confirm this enhancement [51]. If one places the Er^{3+} ions in a Si-nc ridge waveguide (see inset of Fig. 8 right) one can perform experiments on signal amplification at $1.535 \mu\text{m}$ with the aim to demonstrate an Er doped waveguide amplifier (EDWA). The main advantage of an EDWA with respect to an EDFA is the reduced size, the decreased pump power to achieve the same gain, and the wide spectrum range to optically pump the system. A few groups have performed such an experiment [51,55,56].

The most successful result was reported in [55], see Fig. 8 right. In this work a very low Si-nc concentration has been used and an internal gain of 7 dB/cm has been deduced. A successful experiment of pumping the EDWA with LED was also reported [57]. In other experiments, with a large Si-nc concentration, no or weak signal enhancement has been observed [51,56]. The reason is attributed to the presence of a strong confined carrier absorption which introduces a loss mechanism at the signal wavelength and prevents the sensitizing action of the Si-nc. Indeed, the energy transfer is in competition with confined carrier absorption at the signal wavelength (see Fig. 7). A confined carrier cross section of 10^{-18} cm^2 is usually assumed [47]. Propagation losses, saturation of Er^{3+} excitation, up-conversion and confined carrier absorption make difficult the proper design of EDWA where optical amplification can be observed. Having got internal gain, electrically injected LED[54,58] and optical cavities[59], a laser which uses the Er^{3+} -coupled Si-nc system as active material seems feasible. With this respect, it is worth noticing that toroidal microcavities formed in silica doped with Er^{3+} have demonstrated optically pumped lasing at room temperature [60].

5. CONCLUSIONS

After six years since the first observation of optical gain in Si nanocrystals, a first Si laser has been demonstrated, though not using Si-nc but the Raman effect. Various different approaches have been however suggested to achieve electrically pumped lasing in silicon. These cover a wide spectral range spanning from visible to infrared.

- *Silicon bulk based approaches* [$\lambda = 1.2 \mu\text{m}$] aim to increase the non-radiative lifetimes and, hence, to increase the internal quantum efficiency by using passivation or carrier localization either in a small silicon region

or on a point defect. The more successful approaches are based on the use of the nanopatterning of a pn junctions or of a thin silicon layer. Both stimulated emission by electrical injection or by optical pumping at cryogenic temperatures have been observed.

- *Silicon nanocrystals based approaches* [$\lambda = 0.7\mu\text{m}$] aim to beat the indirect band-gap of silicon by using quantum confinement. Both high external quantum efficiency in electroluminescence devices and optical gain under optical pumping have been reported. To achieve electrical pumped optical gain and, hence, lasing one has to control the injection in the silicon nanocrystals so that it becomes bipolar injection. At the same time electrons and holes have to tunnel into the nanocrystals so that efficient recombination is possible. A proper band-gap engineering by changing both the composition and the effective barrier strengths is needed.
- *Er coupled to silicon nanocrystals approaches* [$\lambda = 1.535\mu\text{m}$] where several materials related issue have still to be mastered. Optimization of the deposition parameters, Er content and annealing processes has to be performed by using as figure of merit the waveguide optical gain and not the luminescence intensity as it has been done so far. Once optimization has been reached, the implementation of electrically injected amplifier could be achieved also by using the injection methods suggested for bare Si-nc.

These facts show that the perspectives to achieve an injection laser in Si are nowadays more solids than ever. We are quite optimistic that a laser will be realized in the near future by using one of the various approaches here presented.

Acknowledgements

It is a pleasure to thank the hard work of my coworkers and students. The support of EC through the SEMINANO and SINERGIA projects is also acknowledged.

REFERENCES

1. O. Svelto, D. C. Hanna, Principles of Lasers, Plenum Press, 1998.
2. Ossicini Stefano, Pavesi Lorenzo, Priolo Francesco *Light Emitting Silicon for Microphotonics*, Springer Tracts in Modern Physics, Vol. 194 (Springer-Verlag, Berlin 2003).
3. *Towards the first silicon laser*, edited by L. Pavesi, S. Gaponenko and L. Dal Negro, NATO Science Series (Kluwer Academic Publishers 2003)
4. *Silicon Photonics*, edited by Lorenzo Pavesi and David Lockwood, Topics in Applied Physics vol. 94 (Springer-Verlag, Berlin 2004).
5. P. Jonsson, H. Bleichner, M. Isberg, and E. Nordlander, J. Appl. Phys. **81**, 2256 (1997)
6. Schroder, D. K., R. N. Thomos, and J. C. Swartz, IEEE Trans. Electron. Dev. **ED-25**, 254 (1978)
7. L. Pavesi, L. Dal Negro, C. Mazzoleni, G. Franzò, F. Priolo, Nature **408**, 440 (2000).
8. G. Dehlinger, L. Diehl, U. Gennser, H. Sigg, J. Faist, K. Ensslin, D. Grützmacher Science **290**, 2277 (2000).
9. M. A. Green, J. Zhao, A. Wang, P. J. Reece and M. Gal, Nature **412**, 805 (2001).
10. S. G. Cloutier, P. A. Kossyrev, J. Xu, Nature Materials (2005).
11. O. Boyraz and B. Jalali, Optics Express **12**, 5269 (2004); Optics Express **11**, 1731 (2003) 59; Optics Express **13**, 796 (2005).
12. A. Liu, H. Rong, M. Paniccia, O. Cohen, and D. Hak, Optics Express **12**, 4261 (2004); Nature **433**, 292 (2005); Nature **433**, 625 (2005).
13. J. Zhao, M. A. Green, and A. Wang, J. Appl. Phys. **92**, 2977 (2002).
14. Thorsten Trupke, Martin A. Green, and Peter Wurfel J. Appl. Phys. **93**, 9058 (2003).
15. W. P. Dumke, Phys. Rev. **127**, 1559 (1962).
16. M. J. Chen, J. L. Yen, J. Y. Li, J. F. Chang, S. C. Tsai, and C. S. Tsai Appl. Phys. Lett. **84**, 2163 (2004)
17. M. Zacharias, J. Heitmann, R. Scholz, U. Kahler, M. Schmidt, and J. Bläsing, Appl. Phys. Lett. **80**, 661 (2002).
18. J. Valenta, R. Juhasz, and J. Linnros, Appl. Phys. Lett. **80**, 1070 (2002).

19. N. Daldosso, M. Luppi, S. Ossicini, E. Degoli, R. Magri, G. Dalba, P. Fornasini, R. Grisenti, F. Rocca, L. Pavesi, S. Boninelli, F. Priolo, C. Bongiorno, and F. Iacona, *Phys. Rev. B* **68**, 085327 (2003).
20. Johannes Heitmann, Frank Muller, Lixin Yi, Margit Zacharias, Dmitri Kovalev, Frank Eichhorn, *Phys. Rev. B* **69**, 195309 (2004)
21. L. Khriachtchev, M. Räsänen, S. Novikov, O. Kilpelä, and J. Sinkkonen, *J. Appl. Phys.* **86**, 5601 (1999).
22. Leonid Khriachtchev, Markku Räsänen, Sergei Novikov, Lorenzo Pavesi, *Appl. Phys. Lett.* **85**, 1511 (2004).
23. Y. J. Chabal, Krishnan Raghavachari, X. Zhang, and E. Garfunkel *Phys. Rev. B* **66**, 161315 (2002).
24. J. S. Biteen, N. S. Lewis, and H. A. Atwater A. Polman, *Appl. Phys. Lett.* **84**, 5389 (2004)
25. L. Dal Negro, M. Cazzanelli, N. Daldosso, Z. Gaburro, L. Pavesi, F. Priolo, D. Pacifici, G. Franzò and F. Iacona, *Physica E* **16**, 297 (2003).
26. L. Dal Negro, M. Cazzanelli, L. Pavesi, S. Ossicini, D. Pacifici, G. Franzò, F. Priolo and F. Iacona, *Appl. Phys. Lett.* **82**, 4636 (2003)
27. L. Dal Negro, M. Cazzanelli, B. Danese, L. Pavesi, F. Iacona, G. Franzò and F. Priolo, *J. Appl. Phys.* **96**, 5467(2004).
28. Leonid Khriachtchev, Markku Rasanen, Sergei Novikov, and Juha Sinkkonen, *Appl. Phys. Lett.* **79**, 1249 (2001).
29. J. Ruan, P. M. Fauchet, L. Dal Negro, M. Cazzanelli, and L. Pavesi, *Appl. Phys. Lett.* **83**, 5479 (2003).
30. K. Luterova, K. Dohnalova, V. Svrcek, I. Pelant, J.-P. Likforman, O. Cregut, P. Gilliot, and B. Honerlage, *Appl. Phys. Lett.* **84**, 3280 (2004).
31. M H Nayfeh, S Rao, N Barry, *Appl. Phys. Lett.* **80**, 121 (2002).
32. polarized gain *Phys Rev Lett* (2004)
33. V.I.Klimov, A.A. Mikhailovsky, S. Xu, A. Malko, J. A. Hollingsworth, et al., *Science* **290**, 314, (2000)
34. C. Delerue, M. Lannoo, G. Allan, *Phys. Rev. Lett.* **75**, 2228 (1995).
35. F. Zhou and J. D. Head, *J. Phys. Chem. B* **104**, 981 (2000); A. B. Filonov, S. Ossicini, F. Bassani, F. Arnaud D'Avitaya, *Phys. Rev. B* **65**, 195317 (2002)
36. R.G. Elliman, M.J. Lederer, N. Smith, B. Luther-Davies, *Nucl. Instrum. Methods B* **206**, 427 (2003).
37. A. Mimura, M. Fujii, S. Hayashi, D. Kovalev, F. Koch, *Phys. Rev. B* **62**, 12625 (2000).
38. S. L. Jaiswal et al., *Appl. Phys. A* **77**, 57 (2003).
39. G. Franzò, A. Irrera, E. C. Moreira, M. Miritello, F. Iacona, D. Sanfilippo, G. Di Stefano, P. G. Fallica and F. Priolo, *Appl. Phys. A* **74**, 1 (2002)
40. R. J. Walters, R. I. Bourianof, H. Atwater, *Nature Materials* **4**, 143 (2005).
41. P. Pellegrino, B. Garrido, C. Garcia, J. Arbiol, J.R. Morante, M. Melchiorri, N. Daldosso, L. Pavesi, E. Schedi and G. Sarabayrouse, *J. Appl. Phys.* **97**, 074312 (2005).
42. E. Desurvire, *Erbium-Doped Fiber Amplifiers: Principles and Applications* (Wiley, New York, 1994).
43. G. Franzò, S. Coffa, F. Priolo, C. Spinella, *J. Appl. Phys.* **81**, 2784 (1997).
44. F. Priolo, G. Franzò, S. Coffa, A. Carnera, *Phys. Rev. B* **57**, 4443 (1998).
45. A.J. Kenyon, P.F. Trwoga, M. Federighi, C.W. Pitt, *J. Phys. Condens. Matter* **6**, L319 (1994)
46. M. Fujii, M. Yoshida, Y. Kanzawa, S. Hayashi, K. Yamamoto, *Appl. Phys. Lett.* **71**, 1198 (1997)
47. D. Pacifici, G. Franzò, F. Priolo, F. Iacona, and L. Dal Negro, *Phys. Rev. B* **67**, 245301 (2003)
48. G. Franzò et al., *Appl. Phys. Lett.* **82**, 3871 (2003)
49. D. Kuritsyn, A. Kozanecki, and H. Przybylin'ska, W. Jantsch, *Appl. Phys. Lett.* **83**, 4160 (2003)
50. M. Wojdak et al. *Phys. Rev. B* **69**, 233315 (2004)
51. N. Daldosso, D. Navarro-Urrios, M. Melchiorri, L. Pavesi, F. Goubilleau, M. Carrada, R. Rizk, C. Garcia, P. Pellegrino, B. Garrido, L. Cognolato, *Appl. Phys. Lett.* **86**, 261103 (2005); and submitted to *Applied Physics Letters*.
52. F. Priolo, G. Franzò, D. Pacifici, V. Vinciguerra, F. Iacona, and A. Irrera, *J. Appl. Phys.* **89**, 264 (2001).
53. A. J. Kenyon, C. E. Chryssou, C. W. Pitt, T. Shimizu-Iwayama, D. E. Hole, N. Sharma and C. J. Humphreys *J. Appl. Phys.* **91**, 367 (2002).
54. F. Iacona, D. Pacifici, A. Irrera, M. Miritello, G. Franzò, F. Priolo, D. Sanfilippo, G. Di Stefano, and P. G. Fallica, *Appl. Phys. Lett.* **81**, 3242 (2002).

55. Hak-Seung Han, Se-Young Seo, Jung H. Shin, Namkyoo Park, Appl. Phys. Lett. **81**, 3720 (2002).
56. P. G. Kik and A. Polman, J. Appl. Phys. **91**, 534 (2002).
57. J. Lee, J. Shin, N. Park, "Optical gain in Si-nanocrystal sensitized, Er-doped silica waveguide using top-pumping 470nm LED", Proceedings of Optical fiber communication conference, Los Angeles, CA, 2004
58. Maria Eloisa Castagna., Salvatore Coffa, Mariantonietta Monaco, Anna Muscara, Liliana Caristia, Simona Lorenti, Alberto Messina, Materials Science and Engineering **B105**, 83 (2003).
59. F. Iacona, G. Franzò, E.C. Moreira, F. Priolo: J. Appl. Phys. **89**, 8354 (2001)
60. A. Polman, B. Min, J. Kalkman. T. J. Kippenberg and K. J. Vahala, Appl. Phys. Lett. **84**, 1037 (2004)
61. Kwan Sik Cho et al., Appl. Phys. Lett **86**, 071909 (2005)